HHS Public Access

Author manuscript

J Drug Target. Author manuscript; available in PMC 2016 February 19.

Published in final edited form as:

J Drug Target. 2015 ; 23(0): 750–758. doi:10.3109/1061186X.2015.1076428.

Long-circulating Janus nanoparticles made by electrohydrodynamic co-jetting for systemic drug delivery applications

Sahar Rahmani[1,2,3], **Carlos H. Villa**[4], **Acacia F. Dishman**[1], **Marika E. Grabowski**[1,2], **Daniel C. Pan**[4], **Hakan Durmaz**[1,5], **Asish C Misra**[1,2], **Laura Colón-Meléndez**[1,5], **Michael J. Solomon**[1,5], **Vladimir R. Muzykantov**[4], and **Joerg Lahann**[1,2,3,5]

[1]Biointerfaces Institute, University of Michigan, Ann Arbor, MI, USA

[2]Biomedical Engineering, University of Michigan, Ann Arbor, MI, USA

[3]Institute of Functional Interfaces (IFG), Karlsruhe Institute of Technology (KIT), Germany

[4]Department of Pharmacology, University of Pennsylvania, Philadelphia, PA, USA

[5]Department of Chemical Engineering, University of Michigan, Ann Arbor, MI, USA

Abstract

Background—Nanoparticles with controlled physical properties have been widely used for controlled release applications. In addition to shape, the anisotropic nature of the particles can be an important design criterion to ensure selective surface modification or independent release of combinations of drugs.

Purpose—Electrohydrodynamic (EHD) co-jetting is used for the fabrication of uniform anisotropic nanoparticles with individual compartments and initial physicochemical and biological characterization is reported.

Methods—EHD co-jetting is used to create nanoparticles, which are characterized at each stage with scanning electron microscopy (SEM), structured illumination microscopy (SIM), dynamic light scattering (DLS) and nanoparticle tracking analysis (NTA). Surface immobilization techniques are used to incorporate polyethylene glycol (PEG) and I^{125} radiolabels into the nanoparticles. Particles are injected in mice and the particle distribution after 1, 4 and 24 hours is assessed.

Results and discussion—Nanoparticles with an average diameter of 105.7 nm are prepared by EHD co-jetting. The particles contain functional chemical groups for further surface modification and radiolabeling. The density of PEG molecules attached to the surface of nanoparticles is determined to range between 0.02 and 6.04 ligands per square nanometer. A significant fraction of the nanoparticles (1.2% injected dose per mass of organ) circulates in the blood after 24 h.

Address for correspondence: Professor Joerg Lahann, Director of Biointerfaces Institute, University of Michigan, NCRC, B26, Room 133S, 2800 Plymouth Road, Ann Arbor, MI 48109, USA. Tel: +1 734-763-7543. lahann@umich.edu.

Conclusion—EHD co-jetting is a versatile method for the fabrication of nanoparticles for drug delivery. Circulation of the nanoparticles for 24 h is a pre-requisite for subsequent studies to explore defined targeting of the nanoparticles to a specific anatomic site.

Keywords

Biodistribution studies; electrospraying; functional polymers; Janus nanoparticles; ligand density

Introduction

In the past several decades, there has been a surge of interest in the fabrication, characterization and modification of nanoparticles for a wide range of medical applications including the delivery of therapeutics and imaging of disease components [1–4]. From these studies, it has become clear that a multifaceted approach, where the nanoparticles' design addresses several critical biological barriers that exist from injection to local delivery at the target, is needed to create successful carrier systems [5,6]. Such systems must consider the physical properties of the particles, such as size, shape and texture, as well as the chemical properties such as biodegradability, surface chemistry, charge, targeting groups and stealth moieties [7–9]. Specifically, control over size and surface moieties can have a profound influence over the fate of particles as they travel to the target site [10], while biodegradability and material selection affect the durability of particles in the body and their capability to load and release various therapeutics [11].

A wide range of fabrication methods have been developed to prepare multifunctional particles, including self-assembly of block copolymers [12–14], particle fabrication in non-wetting templates (PRINT) [15], emulsion techniques [16,17], template assisted methods [18,19] and microfluidics [20,21]. Alternatively, electrohydrodynamic (EHD) co-jetting provides a comprehensive design toolbox that allows for the precise control of various particle parameters in order to incorporate the required properties easily and rapidly [22]. In EHD co-jetting, polymeric solutions are processed in a side-by-side flow configuration under laminar conditions. By applying an electric field to the solution, the droplet formed at the tip of the needle is distorted into a Taylor cone. This solution ultimately breaks into a spray of droplets and the rapid evaporation of the solvent induces nano-precipitation and leads to solid particles that are collected on the counter electrode. Due to the rapid nature of the nano-precipitation process, the mixing of the different fluids that make up the jet is suppressed and the EHD process yields particles that are composed of two or more distinct compartments. The compartments can incorporate different functional polymers, which can be functionalized to immobilize targeting, stealth and therapeutic moieties to distinct regions of the particles. Furthermore, each compartment can be loaded with therapeutics and/or imaging agents and their release profiles can be selectively programmed. While other methods can fabricate particles with multiple functionalities, they typically result in isotropic particles where the functionalities are combined in the same area. In contrast, multifunctional particles fabricated through EHD co-jetting can incorporate the different functionalities into distinct regions of the particles, thus resulting in particles where each capability is not compromised.

In the past, we have used the EHD co-jetting technique to fabricate particles from various types of polymers in order to realize different degradation kinetics and/or on-demand capabilities, such as pH-responsive or dual-responsive particles with oxidative and UV triggers, which can be used to control the degradation and release of combinations of therapeutics [23–25]. The incorporation of small molecular weight therapeutics, as well as siRNA and other biomacromolecules, into these multicompartmental particles and their distinct release kinetics have also been studied [23,24,26–28]. Moreover, we have demonstrated the selective and orthogonal surface modification of distinct patches of the particles' surface for incorporation of targeting, stealth or therapeutic moieties [28–32]. Additional work suggests that the precise control of jetting parameters can impart a range of different physical properties such as rod-like or discoid shapes [24,33]. While these factors have a significant effect on the fate of particles in the body and their success as a carrier system, our work has thus far focused mainly on the use of microparticles for these applications, which limits the applicability to specific areas of medicine. The goal of this manuscript is to explore EHD co-jetting for the fabrication of multifunctional nanoparticles and to conduct initial studies of their physicochemical and biological properties. The ability to fabricate nano-sized carriers opens the door to a wide range of applications, where the other functionalities developed thus far by our group can be combined to produce successful carrier systems to combat diseases in which the circulation time of the nanoparticles could have a profound effect on the success of the therapy, such as cancer, cardiovascular diseases, diabetes and Alzheimer's disease [8–10].

Materials and methods

Materials

Chloroform ($CHCl_3$), dimethylformamide (DMF), tetrahydrofuran (THF), 4-(Dimethylamino) pyridine (DMAP), N,N′-Dicyclohexylcarbodiimide (DCC), methanol, pyridinium *p*-toluenesulfonate, 2-methoxypropane triethylamine, acetic acid, sodium acetate, triethyl amine, bromoacetyl bromide, dimethyl amino pyridine, benzyl alcohol, L-lactide, tin (III) ethyl hexanoate, anhydrous toluene, palladium 10% wt. on activated carbon, phosphate buffered saline (PBS), cetyl trimethylammonium bromide (CTAB), copper sulfate pentahydrate, ascorbic acid, poly(4-vinylphenol-*co*-methyl methacrylate) (polymer 2), 4-pentynoic acid, poly[trid(2,5-bis(hexyloxy)-1,4-phenylenevinylene)-*alt*-(1,3-phenylenevinylene)] (PTDPV) and Tween 20 were used as purchased from Sigma Aldrich (St. Louis, MO). *O*-Benzyl-L-serine was purchased from Alfa Aesar (Ward Hill, MA). Sulfuric acid, acetonitrile, sodium nitrite, dichloromethane, sodium carbonate, ProLong Gold anti-fade reagent and acetone were purchased from Fisher Scientific (Waltham, MA). Diethyl ether was purchased from Acros Organics (Morris, NJ) and hydrogen and nitrogen gases were provided by Cryogenic Gases (Detroit, MI). Poly (lactide-*co*-glycolide) (PLGA) with a ratio of 50:50 lactide to glycolide and a molecular weight of 44 and 17 kDa was purchased from Lactel Corporation (Birmingham, AL). ADS 306PT was purchased from American Dye Source, Canada. Azide-polyethylene glycol (PEG)-FITC (mw 3.4 kDa) was purchased from Nanocs (Boston, MA). Eight-arm star PEG (mw 40 kDa) with azide functional groups was purchased from Creative PEG works (Chapel Hill, NC).

Fabrication of nanoparticles

Multicompartmental particles were fabricated through the electrohydrodynamic co-jetting (EHD co-jetting) procedure as previously established in our group [22,30,33]. Briefly, during EHD co-jetting polymer solutions are pumped through syringes tipped with metal needles in a laminar regime, while an electric field is applied to the needles. The solutions form a Taylor cone at the tip of the needles and from this droplet a polymeric jet is ejected towards the collecting electrode. The jet splits into a spray of droplets, where the solvents evaporate rapidly, leaving behind polymeric particles on the counter electrode. To fabricate nanoparticles, polymer solutions composed of a low molecular weight poly(lactide-*co*-glycolide acid) (PLGA 17 kDa, 50:50 lactide:glycolide, 10% w/v) and a surfactant, cetyl trimethylammonium bromide (CTAB, 5% w/v), were used. The solvent system used for EHD co-jetting was a mixture of chloroform and DMF with a ratio of 97:03. The polymer solutions were processed at a flow rate of 0.1 ml/h. In this case, the effects induced by CTAB and the low molecular weight of the polymer resulted in the formation of nanoparticles as opposed to micron-sized particles. The as-fabricated nanoparticles size was determined based on the scanning electron microscopy (SEM) analysis of over 300 nanoparticles using ImageJ software (NIH, Bethesda, MD), while dynamic light scattering (DLS) measurements were used for the analysis of particles after collection and dispersion in buffers and all further modifications.

Structured illumination microscopy

To fabricate nanoparticles for analysis with structured illumination microscopy (SIM, Zeiss, Inc., Portland, OR), different dyes were incorporated into the jetting solutions to enable visualization of each compartment. Here, one compartment contained a polymeric green dye (PTDPV) and one contained a red dye (ADS 306PT). The nanoparticles were jetted directly onto glass coverslips and were incubated in ProLong Gold anti-fade reagent overnight before analysis with SIM.

Polymer 1 synthesis

Hydroxyl functionalized PLGA was synthesized based on a previously established method at a yield of 92% and characterized via GPC and ^{1}H NMR analysis [29]. $M_{n,GPC}$ = 14 870 g/mol; M_w/M_n 1.58 (based on PS standards). ^{1}H NMR (400 MHz, $CDCl_3$, δ): 5.4–4.4 (m, C=OC*H*CH_3O, C*H*CH_2O and C=OC*H*$_2$OC=O), 4.2–3.8 (m, CHC*H*$_2$OH), 1.7–1.5 (bs, C=OCHC*H*$_3$O). Twelve grams of this polymer was dissolved in 100 ml of CH_2Cl_2. 4-Pentynoic acid (2.22 g, 0.022 mol) and DMAP (0.28 g, 2.27 mmol) were added to the solution. After stirring for 10 min at room temperature, DCC (4.69 g, 0.022 mol) dissolved in 30 ml of CH_2Cl_2 was added to the mixture. The reaction mixture was stirred overnight at room temperature under nitrogen. Next, the urea by-product was filtered and the solvent was removed by rotary evaporation. The remaining viscous polymer was dissolved in $CHCl_3$ and precipitated into large amounts of methanol. The dissolution–precipitation procedure was repeated twice to purify the product. After decantation of methanol, the remaining sticky polymer was dissolved in $CHCl_3$ and evaporated to dryness to give the polymer as a light yellow solid. Yield: 12 g (91%). $M_{n,GPC}$ = 10 550 g/mol (based on PS standards). ^{1}H NMR (400 MHz, $CDCl_3$, δ): 5.4–5.3 (m, C*H*CH_2O), 5.2–5.0 (m, C=OC*H*CH_3O), 4.9–4.4 (m,

CHCH_2OC=O and C=OCH_2OC=O), 2.8–2.4 (m, CH≡CCH^2CH_2C=O), 1.96 (s, CH≡CCH_2CH_2C=O), 1.7–1.5 (m, C=OCHCH_3O).

Determining PEG density on nanoparticles

In order to quantify the number of functional groups potentially available for use on the surface of nanoparticles, a fluorescent polyethylene glycol (PEG) was bound to the nanoparticle surface and quantified using the concentration of the PEG and the total surface area of the particles. Nanoparticles with an alkyne functional group on the surface were fabricated using the EHD co-jetting technique described above. Here, 25% w/w of the particle was composed of the alkyne-functionalized PLGA polymer (polymer 1, structure shown in Supplemental Figure S1). To create a more uniform distribution, the nanoparticles were collected after fabrication and separated via centrifugation to yield uniform nanoparticles, the distribution of which was quantified using DLS. The particles were characterized with nanoparticle tracking analysis (NTA) using Nanosight equipment to determine their size distribution as a function of their concentration and were then reacted overnight with increasing concentrations of azide-PEG-FITC (0.01, 0.1 and 1 mg/ml) via copper catalyzed click chemistry (1.3 mg/ml copper sulfate and 5.3 mg/ml of sodium ascorbate). The nanoparticles were centrifuged to separate the particles from the unreacted material and the unreacted azide-PEG-FITC was isolated and measured via UV Visual Spectroscopy at 453 nm to determine the amount of unreacted material, based on a previously established calibration curve. Based on this information, as well as the size distribution and concentration measurements, the total number of PEG molecules reacted per surface area of the nanoparticles was determined.

Fabrication of nanoparticles for *in vivo* injection and their surface modification

To fabricate nanoparticles for biodistribution studies, particles with a phenol-containing polymer (polymer 2, structure shown in Supplemental Figure S1) that could be used for functionalization with I^{125} were fabricated. Here, the versatile EHD co-jetting technique could be modified to incorporate two functional polymers [alkyne containing PLGA polymer (polymer 1) and phenol containing polymethylmethacrylate (PMMA) polymer (polymer 2)] and still result in nanoparticles. In this formulation, the jetting solutions were composed of 50% w/w PLGA 50:50 with a molecular weight of 40 kDa, 25% w/w of polymer 1, and 25% w/w of polymer 2 for a total concentration of 2.5% w/v. Here a lower total concentration was used due to the larger molecular weight of the polymers. The formulation contained CTAB at 1.25% w/v and a ratio of 1:1 for chloroform to DMF, with a flow rate of 0.1 ml/h. After fabrication, the nanoparticles were analyzed via ImageJ analysis to determine their as-fabricated size distribution, then collected and centrifuged to isolate the nanoparticles. The isolated nanoparticles were characterized with DLS and NTA to determine their size distribution and concentrations. To PEG-ylate the nanoparticles, their surfaces were reacted with either a liner or star azide-PEG molecule (25 mg/ml, structures shown in Supplemental Figure S1) via copper catalyzed click chemistry (1.3 mg/ml copper sulfate and 5.3 mg/ml of sodium ascorbate). After the reaction, the particles were washed to remove unreacted material and then incubated in a solution of I^{125} with iodobeads for 3 h to radioactively label them. After the reaction, the particles were washed to remove the unreacted material, then tested both with (i) a TLC, to determine the degree of radioactive

labeling and (ii) a trichloroacetic acid (TCA) assay and measured with a Wallac 1470 Wizard gamma counter, to determine the amount of radioactivity in counts per minutes for specific concentrations of particles [34].

In vivo studies

For all animal experiments, male C57BL/6 mice, 6–8 weeks old, were obtained from Jackson Labs (Las Vegas, NV). Animal experiments, housing and care were performed in accordance with protocols approved by the Institutional Animal Care and Use Committee of the University of Pennsylvania. For all biodistribution experiments, the animals were anesthetized using inhalational isoflurane and injected intravenously via the retro-orbital sinus following a well-established procedure [35,36]. Labeled particles were suspended in 0.9% sodium chloride containing 1% bovine serum albumin by probe sonication immediately prior to injection. Blood was collected by cardiac puncture at the time of sacrifice (1, 4 and 24 h). Three animals were included in each group. At the designated time points, animals were sacrificed and the organs harvested, weighed and counted via a gamma counter (Wizard2, Perkin Elmer). An aliquot of the injection formulation for each particle group was also counted at each time point. Thyroid tissue was collected to assess the presence of free iodine. Data were processed using Prism (GraphPad Software Inc., San Diego, CA) and expressed as the percentage of injected dose per gram of tissue.

Results

Fabrication of nanoparticles via EHD co-jetting and their characterization

Nanoparticles were fabricated via EHD co-jetting (Figure 1), as described in the “Materials and methods” section of this article. In order to obtain nanoparticles rather than larger micron-sized particles, a low-molecular weight PLGA polymer (17 kDa) was used and a charged surfactant (CTAB) was added to the solutions. These conditions resulted in nanoparticles with an average size of 423 ± 291.46 nm as measured by ImageJ analysis of SEM images (Figure 1). To demonstrate the bicompartmental nature of the nanoparticles, SIM was employed. Here, bicompartmental particles with a red dye in one compartment and a green dye in the second compartment were imaged via a Zeiss SIM (Figure 2). The inset images of individual particles clearly establish the bicompartmental nature of the particles, as the two dyes do not overlap and occupy distinct regions of the particles.

Determining PEG density on the surface of nanoparticles

To further functionalize the nanoparticles, the incorporation of functional polymers for the immobilization of various moieties to the surfaces of the particles was pursued. Here, the same formulation was employed as for the basic nanoparticles, but 25% w/w of the base polymer (i.e. PLGA) was substituted with an alkyne-functionalized PLGA derivative (polymer 1) with a similar molecular weight (see the “Materials and methods” section for a detailed experimental procedure and analysis of polymer 1). The particles were slightly smaller in size compared to their non-functionalized counterparts as indicated by an average size of 311 ± 145.6 nm. To obtain a monodispersed population of nanoparticles, the samples were fractionated by centrifugation. After centrifugation, the average size of the nanoparticles was 161.5 ± 33 nm based on NTA of over 0.23 billion nanoparticles. Based on

the NTA analysis, which gives the concentration of particles at specific diameters, the total surface area of the nanoparticles per ml of solution was calculated.

To determine the ability of molecules to be attached to the surface of these particles and to quantify the attachment density, fluorescent PEG molecules (azide-PEG-FITC) were immobilized to the surface of the particles via copper-catalyzed click reaction. Here, two sets of particles, one with alkyne functional groups on both hemispheres (i.e. monocompartmental) and one with alkyne functional groups on one side only (i.e. bicompartmental) were used. After the reaction, the samples were centrifuged to collect the particles and the unreacted fluorescent PEG molecules that remained in the supernatant were measured via UV Visual Spectroscopy. Based on a previously established calibration curve, the amount of PEGs attached to the surface of the nanoparticles was determined. Combining this information with the surface area data determined by the NTA analysis, the number of PEG molecules attached per square nanometer could be determined. Figure 3 illustrates this data for both monocompartmental and bicompartmental nanoparticles for three different concentrations of the azide-PEG-FITC molecule (0.01, 0.1 and 1 mg/ml). In the case of particles with two active compartments, the ligand density increased with increasing PEG concentration from 0.02 to 6.04 ligands per square nanometer. The same trend was observed for the nanoparticles with one active compartment, with the distinction that at higher concentrations the ligand density of the bicompartmental nanoparticles is significantly lower (3.67 ligands per square nanometer) due to the fact that only one hemisphere is covered with the ligand.

Fabrication of nanoparticles with dual functionalities and their surface modifications

With the establishment of a surface modification procedure for bicompartmental nanoparticles, the specific functionalization of nanoparticles for subsequent biodistribution studies in animals was pursued. Nanoparticles containing polymer 1 designed for surface functionalization with PEG molecules and a second, phenol-containing polymer (polymer 2), designed for radioactive labeling with I^{125}, were prepared (Figure 4). The base polymer was a biodegradable PLGA and each of the functional polymers was added at a ratio of 25% (w/w). A scheme highlighting the chemical route used for functionalization of the nanoparticles, SEM images of particles obtained directly after EHD co-jetting, and their size distributions before and after modification with both linear and star azide-PEG based on DLS analysis are shown in Figure 4. The nanoparticles ranged from 22 to 201 nm in diameter and had an average size of 74.2 ± 30.7 nm directly after fabrication as measured by ImageJ analysis, which is more uniform as compared to the unmodified nanoparticles. The nanoparticles were centrifuged to remove any potential aggregates. Based on DLS analysis, the size of the nanoparticles after centrifugation averaged 105.7 nm, which increased to 122.4 nm after the attachment of linear PEG. In addition to the increase in size due to the hydrophilic layer of the PEG, the size distribution further narrowed from a width of 204.3 to 98.8 nm. The nanoparticles functionalized with the eight-arm PEG molecules increased in size to 164.2 nm while their width of distribution narrowed to 48.3 nm. We note that these nanoparticles were prepared at exceptionally high yields of 51.7 trillion nanoparticles per ml, which translates into a production rate of 17 trillion nanoparticles per hour.

In vivo biodistribution of PEG-ylated nanoparticles in mice

For biodistribution studies in mice, nanoparticles with both functionalities (polymer 1 and 2) were fabricated, isolated via centrifugation, PEG-ylated with star PEG-azide through copper catalyzed click chemistry with the alkyne groups of polymer 1, and analyzed with DLS for size distribution (Figure 5A). After further purification, the nanoparticles were incubated with I^{125} and iodobeads to radioactively label the nanoparticles through immobilization using the phenol groups of polymer 2. After the reaction and purification via centrifugation, a TLC analysis of the nanoparticle solutions was done to determine the amount of I^{125} attached to the nanoparticles. Based on this analysis, 94.7% of the I^{125} in the final samples were attached to the nanoparticles. The nanoparticles (2.5 trillion in 100 μl) were then injected intravenously via the retro-orbital sinus into mice. The animals were sacrificed after 1, 4 and 24 h, their blood was collected via a cardiac puncture, and their different organs were harvested, weighed, and counted via a gamma counter (Wallac 1470 Wizard, Perkin Elmer, Waltham, MA). Based on these measurements, the amount of radioactivity (Percent of Injected Dose – ID%) per gram of tissue present (g) was determined (Figure 5B). As expected of non-targeted nanoparticles, the majority of the samples were found in the liver and spleen, with 41.06 and 55.58% ID/g after one hour and 35.09 and 29.89% ID/g after 24 h, respectively. The particles were also present in significant concentrations in the lungs (20.99 and 2.18% ID/g), kidney (2.05 and 0.95% ID/g), stomach (9.15 and 0.28% ID/g), and bones (2.32 and 1.94% ID/g) after one and 24 h, respectively. Importantly, a significant amount of the particles were present in the blood after one hour and 24 h at 3.8 and 1.1% ID/g, respectively. In addition, the thyroid tissue contained 0.5, 1.4 and 1.4% of the injected dose at 1, 4 and 24 h, suggesting minimal amounts of free iodine were present.

Discussion

The ability to fabricate nanoparticles and to impart distinct functionalities to them is a key factor in manufacturing effective carrier systems. EHD co-jetting can be employed to fabricate particles with a wide range of capabilities and properties due to the versatility and flexibility of the fabrication method. Here, we have combined some of our previously established methodologies with respect to fabricating multicompartmental particles and their distinct surface modifications with new fabrication techniques to produce uniform nanoparticles with distinct surface patches that are used for the incorporation of stealth and imaging capabilities.

To fabricate nanoparticles, a low molecular weight PLGA polymer and a charged surfactant (CTAB) were employed (Figure 1). The corresponding change in the jetting solution parameters, especially the dielectric constant, resulted in the fabrication of sub-micron nanoparticles that ranged in size from 100 to 1000 nm. These nanoparticles contained individual compartments that were visualized using SIM imaging, where each compartment contained a different dyed polymer. SIM imaging was used as opposed to typical confocal microscopy due to the small size of the nanoparticles and the size-associated limits of confocal microscopy. As observed in Figure 2, the individual nanoparticles contained two distinct regions occupied by red or green fluorescence, confirming the compartmental nature of the nanoparticles.

Once the fabrication of nanoparticles at the 100 nm scale and their compartmental nature were established, incorporation of functional polymers into the system for further surface modifications was pursued. Polymer 1, an alkyne-functionalized PLGA, was synthesized by replacing the functional groups of a hydroxyl-containing PLGA, previously published by our group, with alkyne molecules via DCC chemistry [29]. The final product, polymer 1, was purified and fully characterized. Polymer 1 had a similar molecular weight to the PLGA used to make the nanoparticles and could thus be incorporated directly into the jetting solution at the same concentration. To determine the degree to which these functional groups could be used to create specific patches, nanoparticles were fabricated with polymer 1 in either one or both compartments. The nanoparticles were centrifuged after collection to create a more uniform sample and a fraction with an average size of 161.5 ± 33 nm was isolated. The particles were analyzed with DLS to determine their size distribution and NTA to determine their concentration with respect to individual diameters. The density of functional groups on the surface of the particles could then be studied by reacting the surface groups with a fluorescent tag that could be measured via UV Visual Spectroscopy. Here, an azide-PEG-FITC was used as the probe, where the molecule was attached to the surface via copper catalyzed click chemistry. By measuring the amount of unreacted material and taking into account the total surface area of the nanoparticles based on the NTA measurements, the density of the PEG molecules on the surface of the particles in terms of ligand number per surface area could be determined. As would be expected, by increasing the concentration of the reacting material (fluorescent PEG), the ligand density increased from 0.02 to 6.04 ligands per square nanometer for the monophasic particles. This corresponds well with other reported data in literature, which report a range of 4.2–28.5 ligands per square nanometer depending on the type of particles and reactants used [37,34]. For the bicompartmental nanoparticles (with one active surface), a similar trend can be observed, where the number of ligands increases from 0.02 to 3.67 ligands per square nanometer. The significance here is the distinct difference in ligand density at the higher concentrations closer to the saturation point of the functional groups on the surface, which demonstrates that the nanoparticles are indeed bicompartmental and contain a specific patch on their surface.

As mentioned previously, EHD co-jetting is a versatile method and its various parameters can be modified to incorporate different materials, whether polymer or therapeutics, into the particles. In order to incorporate imaging capabilities, polymer 2 [poly(4-vinylphenol-*co*-methyl methacrylate)], a phenol-containing polymer, was incorporated into the nanoparticles. To create nanoparticles, the formulation was altered to include a higher molecular weight PLGA polymer and a higher ratio of DMF in the solvent system in addition to the charged surfactant. The fabricated nanoparticles were more uniform in size than their predecessors (Figure 4B) directly after jetting and averaged at 105.7 nm after centrifugation based on DLS analysis (Figure 4C). While the size distribution was more uniform in this case, some of the nanoparticles aggregated due to the hydrophobic nature of PLGA. This size distribution narrowed as the surface was functionalized with a hydrophilic PEG layer, going from a width of 204.3 nm for unfunctionalized nanoparticles to 98.8 nm for nanoparticles with a linear PEG and 48.3 nm for nanoparticles with a star PEG as aggregations were further reduced. As demonstrated in Figure 4(C), the size of the nanoparticles also increased from 105.7 (unmodified) to 122.4 (linear PEG), and then to

164.2 nm (star PEG) as the PEG layer became more dense in going from linear to star shaped PEGs (5–40 kDa). The size distribution, and especially the resulting reduction in aggregation, is a key factor in manufacturing nanoparticles for drug delivery due to their direct impact on circulation times and clearance (larger particles and more hydrophobic particles are cleared more rapidly by macrophages) [38,39].

After establishing the particle PEG-ylation procedures and their fabrication in high yields (trillions of nanoparticles per hour), further functionalization of the nanoparticles with I^{125} and their biodistribution in mice were studied. For biodistribution studies, the nanoparticles functionalized with star PEG and an average size of 194.6 ± 25.7 nm were employed (Figure 5A). To label the nanoparticles for radioactive detection with a gamma counter, a previously published method was used where the nanoparticles were incubated with I^{125} and iodobeads to attach the I^{125} to the phenol groups of the nanoparticles through the electrophilic aromatic substitution wherein the iodione is inserted in the ortho position to the hydroxyl group of the phenol molecule (Figure 4A) [40]. The I^{125} substitution allows for detection in animal models via gamma counters and I^{124} incorporation can be used for the detection of beta emitters using positron emission tomography (PET) or single photon emission computer tomography (SPECT) imaging [40]. For these studies, we focused on the immobilization of I^{125} on the particles in order to enable the detection is specific organs using gamma counters. After attachment, the nanoparticles were purified from unreacted materials through multiple centrifugations washes before inserting them into animals intravenously via the retro-orbital sinus. The animals were sacrificed at 1, 4 and 24 h periods and their various organs were analyzed to determine the distribution of the nanoparticles within them as a function of the injected dose (ID) per mass of organ (g) (Figure 5B). As a note, the animals were not perfused with a buffer before taking the measurements and each organ contained its respective blood supply. Not surprisingly, the majority of nanoparticles accumulated in the liver and spleen (35.09 and 29.89% ID/g after 24 h, respectively), especially since these nanoparticles were not targeted to a specific site in the body. However, a significant portion of the nanoparticles (approximately 4% ID/g) continued to circulate after one hour, which dropped to 1.2% ID/g even after 24 h. This distribution compares well with published results of similar nanoparticles fabricated through the double emulsion technique where less than 1% ID/g of PEG-ylated nanoparticles were seen after 12 h [41]. The continued circulation of these nanoparticles even after 24 h are promising results, especially considering that further modification of these nanoparticles to incorporate targeting moieties could potentially result in better targeted carrier systems.

Conclusions

Electrohydrodynamic co-jetting is a versatile method for the fabrication of multicompartmental nanoparticles with desirable physical and biological properties. In this article, the fabrication of nanoparticles with sizes below 100 nm through varying critical process parameters (polymer composition, concentration, surfactants or solvent ratios) was pursued. Multicompartmental nanoparticles with multiple functionalities were fabricated and their size distribution, bicompartmental nature and surface ligand densities were determined. The functional groups present on the surface of the nanoparticles were used for the immobilization of a stealth moiety (PEG-azide via copper click chemistry with the alkyne

groups on the particles) and a radioactive molecule (I^{125} via incorporation into the phenol groups on the particles) to enable tracking in animals. Circulation of these nanoparticles in mice persisted over 24 h indicating a potential use for various drug delivery applications. Bicompartmental nanoparticles have the potential to be successful carriers for therapeutics and imaging agents for a multitude of diseases, especially since their surfaces can be further modified to include targeting capabilities that can enhance their effectiveness as drug delivery vehicles.

Supplementary Material

Refer to Web version on PubMed Central for supplementary material.

Acknowledgments

Declaration of Interest

The authors would like to acknowledge funding from the Multidisciplinary University Research Initiative of the Department of Defense and the Army Research Office (W911NF-10-1-0518), the DOD through an idea award (W81XWH-11-1-0111), the Tissue Engineering and Regenerative Medicine Training Grant (DE00007057-36), and the European Community's Seventh Framework Programme (FP7/2007-2013) under grant agreement n^{o} 310445 (SAVVY).

References

1. Wicki A, Witzigmann D, Balasubramanian V, Huwyler J. Nanomedicine in cancer therapy: challenges, opportunities, and clinical applications. J Control Release. 2015; 200:138–57. [PubMed: 25545217]
2. Lim EK, Kim T, Paik S, et al. Nanomaterials for theranostics: recent advances and future challenges. Chem Rev. 2015; 115:327–94. [PubMed: 25423180]
3. Sun TM, Zhang YS, Pang B, et al. Engineered nanoparticles for drug delivery in cancer therapy. Angew Chem Int Ed. 2014; 53:12320–64.
4. Brigger I, Dubernet C, Couvreur P. Nanoparticles in cancer therapy and diagnosis. Adv Drug Deliv Rev. 2002; 54:631–51. [PubMed: 12204596]
5. Neffe AT, Lendlein A. Going beyond compromises in multi-functionality of biomaterials. Adv Healthc Mater. 2015; 4:642–5. [PubMed: 25546324]
6. Sailor MJ, Park JH. Hybrid nanoparticles for detection and treatment of cancer. Adv Mater. 2012; 24:3779–802. [PubMed: 22610698]
7. Mu QX, Jiang GB, Chen LX, et al. Chemical basis of interactions between engineered nanoparticles and biological systems. Chem Rev. 2014; 114:7740–81. [PubMed: 24927254]
8. Shi DL, Bedford NM, Cho HS. Engineered multifunctional nanocarriers for cancer diagnosis and therapeutics. Small. 2011; 7:2549–67. [PubMed: 21648074]
9. Morachis JM, Mahmoud EA, Almutairi A. Physical and chemical strategies for therapeutic delivery by using polymeric nanoparticles. Pharmacol Rev. 2012; 64:505–19. [PubMed: 22544864]
10. Peer D, Karp JM, Hong S, et al. Nanocarriers as an emerging platform for cancer therapy. Nat Nanotechnol. 2007; 2:751–60. [PubMed: 18654426]
11. Kost J, Langer R. Responsive polymeric delivery systems. Adv Drug Deliv Rev. 2001; 46:125–48. [PubMed: 11259837]
12. Walther A, Andre X, Drechsler M, et al. Janus discs. J Am Chem Soc. 2007; 129:6187–98. [PubMed: 17441717]
13. Kim JW, Larsen RJ, Weitz DA. Synthesis of nonspherical colloidal particles with anisotropic properties. J Am Chem Soc. 2006; 128:14374–7. [PubMed: 17076511]
14. Higuchi T, Tajima A, Motoyoshi K, et al. Frustrated phases of block copolymers in nanoparticles. Angew Chem Int Ed. 2008; 47:8044–6.

15. Perry JL, Herlihy KP, Napier ME, Desimone JM. PRINT: a novel platform toward shape and size specific nanoparticle theranostics. Acc Chem Res. 2011; 44:990–8. [PubMed: 21809808]
16. Cho YS, Yi GR, Kim SH, et al. Particles with coordinated patches or windows from oil-in-water emulsions. Chem Mater. 2007; 19:3183–93.
17. Zhang J, Jin J, Zhao HY. Surface-initiated free radical polymerization at the liquid-liquid interface: a one-step approach for the synthesis of amphiphilic Janus silica particles. Langmuir. 2009; 25:6431–7. [PubMed: 19466790]
18. Jiang S, Chen Q, Tripathy M, et al. Janus particle synthesis and assembly. Adv Mater. 2010; 22:1060–71. [PubMed: 20401930]
19. Zhou T, Wang BB, Dong B, Li CY. Thermoresponsive amphiphilic Janus silica nanoparticles via combining “polymer single-crystal templating” and “grafting-from” methods. Macromolecules. 2012; 45:8780–9.
20. Wang JT, Wang J, Han JJ. Fabrication of advanced particles and particle-based materials assisted by droplet-based microfluidics. Small. 2011; 7:1728–54. [PubMed: 21618428]
21. Dendukuri D, Doyle PS. The synthesis and assembly of polymeric microparticles using microfluidics. Adv Mater. 2009; 21:4071–86.
22. Roh KH, Martin DC, Lahann J. Biphasic Janus particles with nanoscale anisotropy. Nat Mater. 2005; 4:759–63. [PubMed: 16184172]
23. Rahmani S, Park TH, Dishman AF, Lahann J. Multimodal delivery of irinotecan from microparticles with two distinct compartments. J Control Release. 2013; 172:239–45. [PubMed: 23973814]
24. Misra AC, Bhaskar S, Clay N, Lahann J. Multicompartmental particles for combined imaging and siRNA delivery. Adv Mater. 2012; 24:3850–6. [PubMed: 22581730]
25. Sokolovskaya E, Rahmani S, Misra AC, et al. Dual stimuli responsive microparticles. ACS Appl Mater Interfaces. 2015; 7:9744–51. [PubMed: 25886692]
26. Hwang S, Lahann J. Differentially degradable Janus particles for controlled release applications. Macromol Rapid Commun. 2012; 33:1178–83. [PubMed: 22605558]
27. Park TH, Eyster TW, Lumley JM, et al. Photoswitchable particles for on-demand degradation and triggered release. Small. 2013; 9:3051–7. [PubMed: 23606461]
28. Rahmani S, Ross AM, Park TH, et al. Dual release carriers for cochlear delivery. Adv Healthc Mater. 2015 [Epub ahead of print]. DOI: 10.1002/adhm.201500141.
29. Rahmani S, Saha S, Durmaz H, et al. Chemically orthogonal three-patch microparticles. Angew Chem Int Ed. 2014; 53:2332–8.
30. Bhaskar S, Roh KH, Jiang XW, et al. Spatioselective modification of bicompartmental polymer particles and fibers via Huisgen 1,3-dipolar cycloaddition. Macromol Rapid Commun. 2008; 29:1655–60.
31. Bhaskar S, Hitt J, Chang SWL, Lahann J. Multicompartmental microcylinders. Angew Chem Int Ed. 2009; 48:4589–93.
32. Sokolovskaya E, Yoon J, Misra AC, et al. Controlled micro-structuring of Janus particles based on a multifunctional poly(ethylene glycol). Macromol Rapid Commun. 2013; 34:1554–9. [PubMed: 23982931]
33. Bhaskar S, Pollock KM, Yoshida M, Lahann J. Towards designer microparticles: simultaneous control of anisotropy, shape, and size. Small. 2010; 6:404–11. [PubMed: 19937608]
34. Liu HY, Doane TL, Cheng Y, et al. Control of surface ligand density of PEGylated gold nanoparticles for optimized cancer cell uptake. Part Part Syst Char. 2014; 32:197–204.
35. Yardeni T, Eckhaus M, Morris HD, et al. Retro-orbital injections in mice. Lab Animal. 2011; 40:155–60. [PubMed: 21508954]
36. Nanni C, Pettinato C, Ambrosini V, et al. Retro-orbital injection is an effective route for radiopharmaceutical administration in mice during small-animal PET studies. Nucl Med Commun. 2007; 28:547–53. [PubMed: 17538396]
37. Hinterwirth H, Kappel S, Waitz T, et al. Quantifying thiol ligand density of self-assembled monolayers on gold nanoparticles by inductively coupled plasma-mass spectrometry. ACS Nano. 2013; 7:1129–36. [PubMed: 23331002]

38. Bertrand N, Leroux JC. The journey of a drug-carrier in the body: an anatomo-physiological perspective. J Control Release. 2012; 161:152–63. [PubMed: 22001607]

39. Moghimi SM, Hunter AC, Andresen TL. Factors controlling nanoparticle pharmacokinetics: an integrated analysis and perspective. Annu Rev Pharmacol. 2012; 52:481–503.

40. Simone EA, Zern BJ, Chacko AM, et al. Endothelial targeting of polymeric nanoparticles stably labeled with the PET imaging radioisotope iodine-124. Biomaterials. 2012; 33:5406–13. [PubMed: 22560201]

41. Li YP, Pei YY, Zhang XY, et al. PEGylated PLGA nanoparticles as protein carriers: synthesis, preparation and biodistribution in rats. J Control Release. 2001; 71:203–11. [PubMed: 11274752]

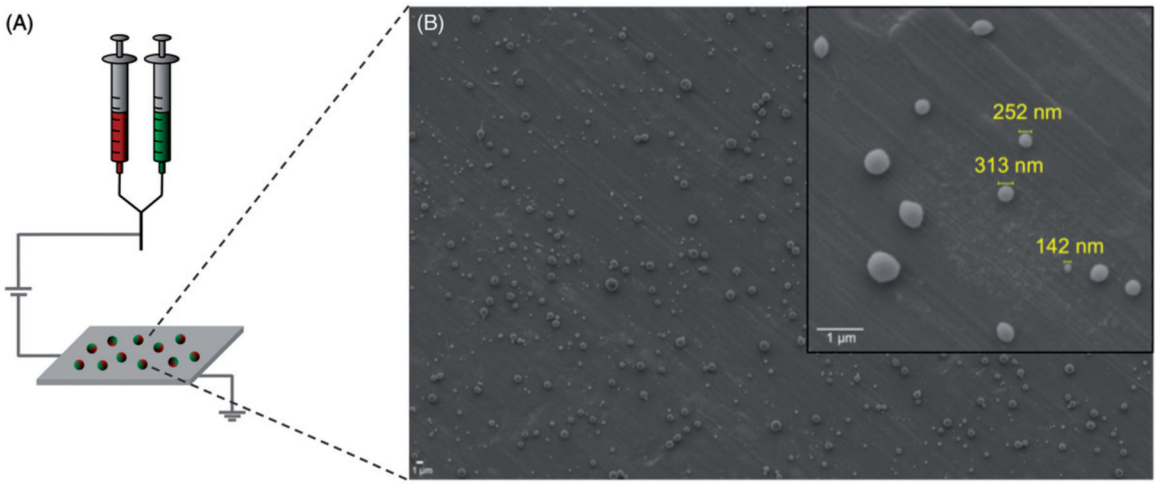

Figure 1.

Fabrication of nanoparticles via the EHD co-jetting. (A) Schematic of the EHD co-jetting system and (B) representative SEM image of nanoparticles fabricated by this method. All scale bars are 1 μm.

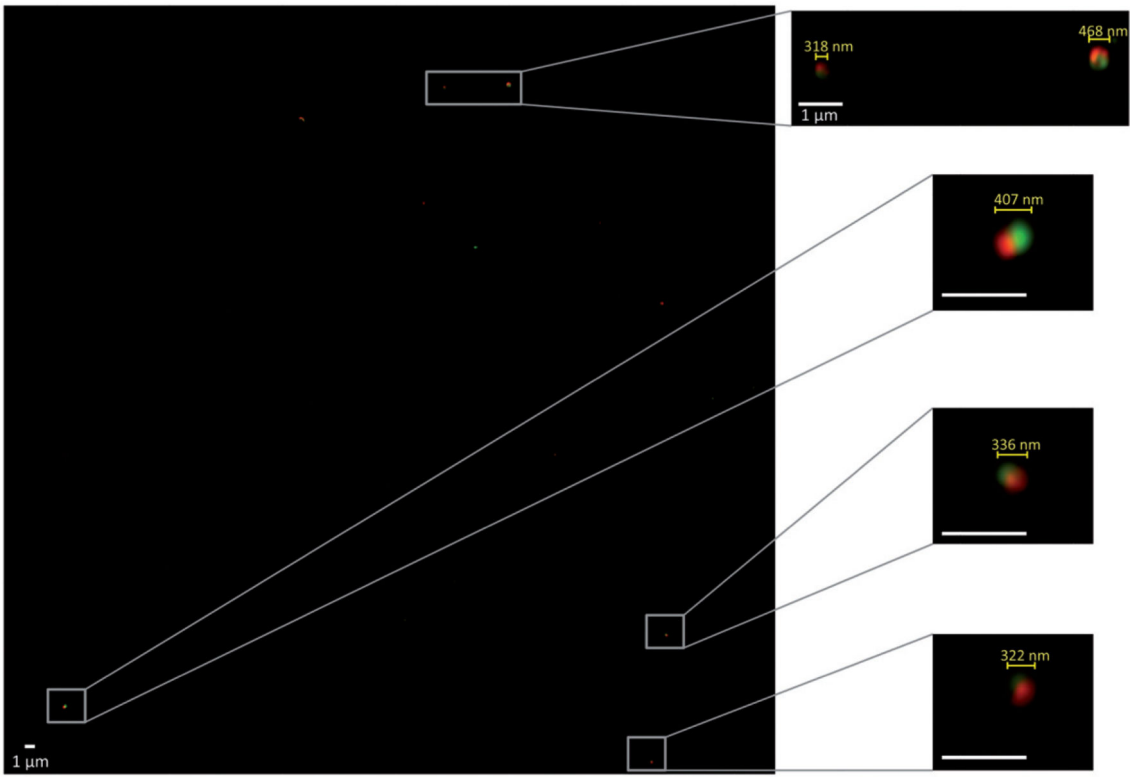

Figure 2.

Structured illumination microscopy (SIM) images of nanoparticles with two distinct compartments containing a red or green dye. The left image is a wide scan of the entire area and select particles are shown at a higher magnification on the right to demonstrate the compartmental nature of the particles. All scale bars are 1 μm.

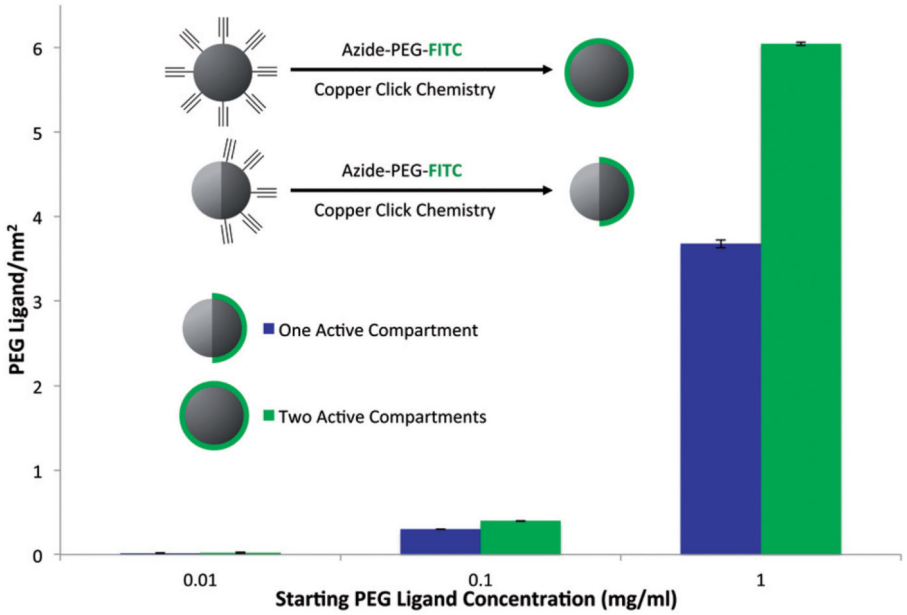

Figure 3.

Determining PEG density on the surface of nanoparticles. Monophasic or Janus particles with a functional polymer on the entire surface or one hemisphere, respectively, were reacted with azide-PEG-FITC and the PEG ligand per area was determined for each sample.

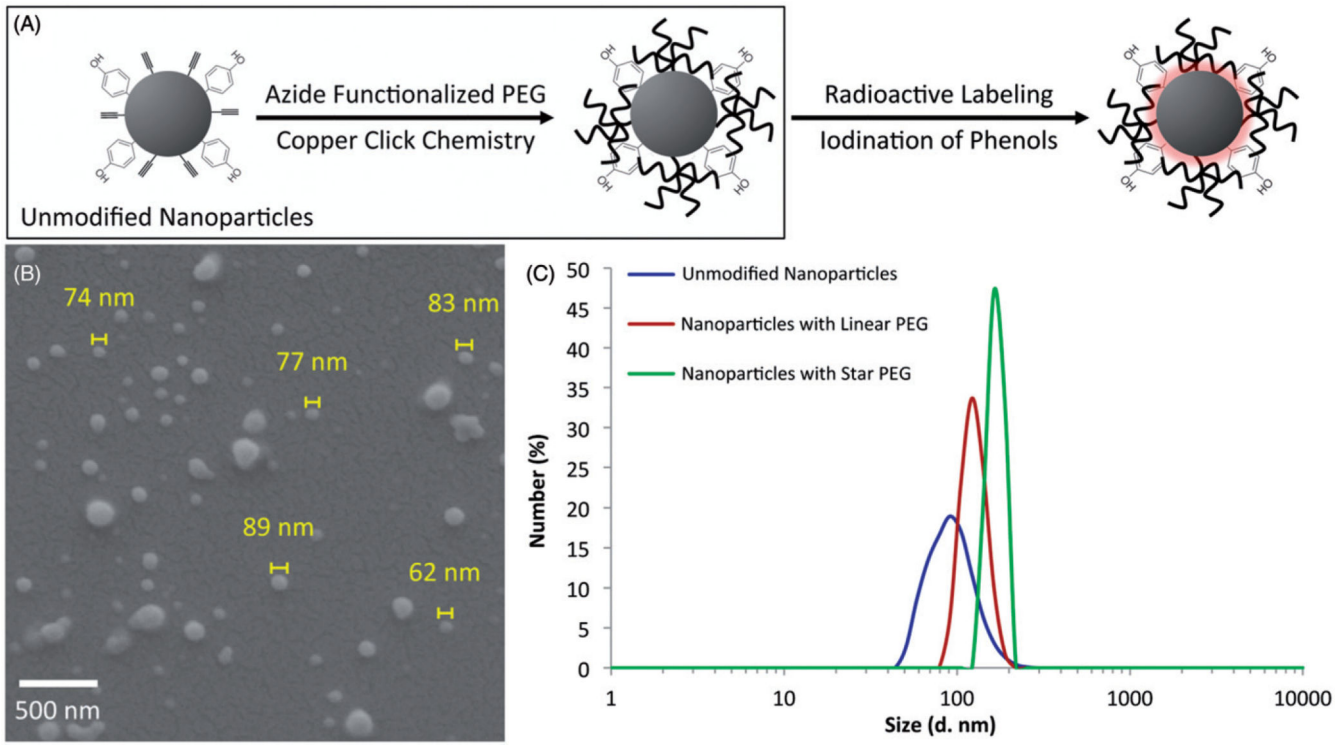

Figure 4.

Fabrication of nanoparticles with phenol and alkyne functional groups and their size distribution after surface modification. (A) The schematic of the surface modifications used and the surface functional groups present on the nanoparticles. (B) The as-fabricated nanoparticles containing both functional polymers and (C) the size distribution of the particles after collection and surface modification with linear or star PEG molecules. The scale bar in (B) is 500 nm.

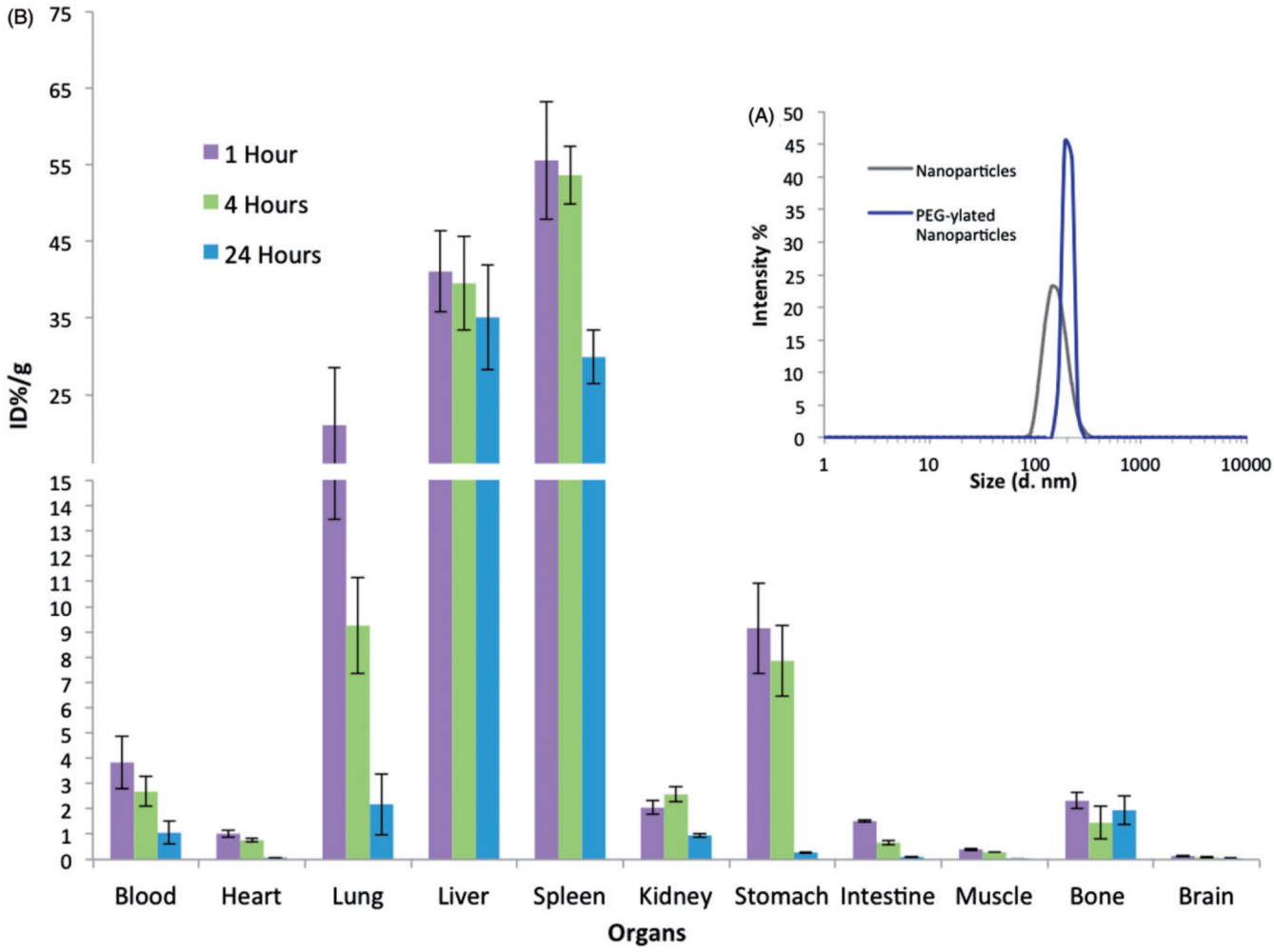

Figure 5.

Biodistribution of nanoparticles in mice. (A) The size distribution of the collected and star PEG-ylated nanoparticles based on DLS analysis and (B) the nanoparticle biodistribution in different organs at 1, 4 and 24 h are demonstrated in (C).